A novel approach for regulation of the diffusive effects of limiters in viscous-compressible-flow computations using a boundary-layer sensor

†*Anoop Kumar Dass[1], and Paragmoni Kalita[2]

[1]Professor, Department of Mechanical Engineering, I.I.T. Guwahati. Assam, India-781039
[2]Assistant Professor, Department of Mechanical Engineering, Tezpur University, Assam, India-784028

*Presenting author: anoop@iitg.ernet.in
†Corresponding author: anoop@iitg.ernet.in

Abstract

Accurate computations of high-speed-viscous flows demand the use of higher-order-accurate schemes for computing the inviscid-flux vectors. However, the constraint of monotonicity preservation calls for the need of limiters in the solution or flux reconstructions used for obtaining higher-order accuracy. The necessity for use of limiters is strong in the inviscid-flow regions owing to the presence of discontinuities like shocks, contact surfaces, slip lines etc. In contrast, the flow field inside the boundary layer is smoother compared with that outside the shear layer in viscous-compressible flows. It is a well-known fact that all the limiters inherently possess diffusive effects like extremum clipping. These diffusive effects of limiters add up with the physical dissipation present inside the boundary layer and spoil the solution accuracy. To overcome this problem, this paper proposes a novel approach to control the limiters used for MUSCL reconstruction using a recently introduced boundary layer sensor. The limiters are switched off inside the boundary layer using the sensor. This approach results in controlling the diffusive effects of the limiters in the higher-order-accurate computation of viscous-compressible flows. The higher accuracy of the new methodology is demonstrated by a number of carefully selected test problems using van Albada limiter.

Keywords: **MUSCL, reconstruction, limiter, boundary layer sensor**

Introduction

The design of accurate, robust and efficient schemes for computing high-speed flows has been an area of prime importance in the field of computational gasdynamics [1]. The dynamics of inviscid-compressible flows is governed by the Euler equations of gasdynamics. Even for high-speed viscous applications governed by the compressible Navier-Stokes equations, the convective fluxes are numerically computed by using the same flux formulas developed for the Euler equations. The design of a stable and accurate numerical scheme for the convective fluxes is a highly challenging task because the highly nonlinear behaviour of these equations admits discontinuous solutions in the forms of shocks, contact discontinuities, slip surfaces, and also expansion waves with sonic points [2]. Since the unsteady Euler equations are hyperbolic in nature admitting wave-like solution, simple central differencing of the fluxes leads to numerical instabilities necessitating the development of upwind schemes which comprise one-sided differencing that respects the direction of signal propagation. Roe's Flux-Difference Splitting (FDS) [3], van Leer's Flux-Vector Splitting (FVS) [4], Liou and Steffen's Advection Upstream Splitting Method (AUSM) [5], Nishikawa and Kitamura's Rotated Riemann Solvers [6], Residual Distribution (RD) schemes [7-8], multidimensional Riemann solvers [9-12] are examples of some popular upwind methods. It can be shown that an upwind scheme is equivalent to central-space discretization plus an "implicit" numerical diffusion term. In other words, addition of numerical diffusion plays the role of imparting stability to a purely central space discretization of the convective-flux vectors. Contrary to the upwind schemes, the central schemes choose a symmetric stencil irrespective direction of signal propagation. For numerical stability some artificial diffusion is added to the central-space discretization of the flux. The Lax-Friedrichs [13], Lax-Wendroff [14], Local-Lax Friedrichs [15], Jameson-Schmidt-Turkel (JST) [16] are to mention a few noteworthy central schemes.

While numerical diffusion is essential for stability, excessive diffusion spoils the solution accuracy by smearing the discontinuities and shear layers. Especially for viscous-flow computations excessive numerical diffusion causes the smearing of boundary layers, under prediction of skin friction and wall-heat fluxes [5, 17, 18] and over-prediction of separation-bubble sizes [19]. For example, though van Leer's FVS scheme is robust and accurate for the computation of the Euler equations, it is less accurate than AUSM for viscous-flow computations owing to the more diffusive nature of the former [5]. It may be noted that the numerical diffusion required for stability is high in zones of shocks or sharp gradients, while in smooth-flow regions its requirement is less. These requirements call for the regulation of numerical diffusion based on the smoothness of flow field.

Godunov showed that a monotonous conservative linear scheme can be at best first-order accurate [20]. However, because of excessive numerical diffusion the first-order accurate computations are not preferred for viscous-flow computations. Naturally for accurate computation of viscous flows one needs to go for higher-order-accurate schemes. Nevertheless, the higher-order-accurate reconstructions of the fluxes require the use of nonlinear limiters in order to avoid spurious numerical oscillations [21 (van Leer, 1979)]. The limiters aid in the attainment of monotonous solutions, but they also induce diffusive effects like extremum clipping [22]. Kalita and Dass [18] presented an improved version of the Diffusion-Regulated Local Lax Friedrichs (DRLLF) scheme [23] for viscous computations by scaling down its numerical diffusion inside the boundary layer using a new boundary-layer sensor with different limiters in the higher-order reconstructions.

In viscous flows solution gradients may exist inside the boundary layers. However, these gradients are mild owing to the diffusive effects of physical viscosity. Therefore, a scope exists to control the diffusive effects of limiters inside shear layers in the computation of viscous-compressible flows. To the best of our knowledge, efforts to suppress the action of limiters inside the boundary layers are not reported in the available literature. This work presents a novel approach of controlling the limiters only inside the boundary layers in computations of high-speed-viscous flows on a finite volume framework. This approach switches off the limiters inside the viscous-shear layers using a recently introduced boundary layer sensor [18]. Outside the boundary layer the original-solution-reconstruction approach with full limiting is followed. For the demonstration, the performance of higher-order-accurate AUSM scheme with MUSCL reconstruction [21] using the van Albada limiter [24 (van Albada)] is shown for a number of viscous supersonic and hypersonic test cases. The numerical experiments reveal that the new approach of controlling the diffusive effects of limiters produces more accurate results compared with the higher-order versions of the same scheme with full limiting over the entire flow field.

This paper is organized in four sections. The next section presents the numerical methodology for computing the boundary-layer sensor and an algorithm for controlling the limiters using the same. The improved performance of the new approach is demonstrated in the section on "Numerical Simulations, Results and Discussion" with a number of standard-test cases, before making the concluding remarks in the "Conclusions" section.

The numerical methodology and the algorithm to control limiters

We first introduce the MUSCL reconstruction for a one-dimensional (1D) formulation. The same methodology can be easily extended to multiple dimensions. A 1D-computational domain is shown in Fig. 1. The left and right states for any variable U across any cell-interface $I+\frac{1}{2}$ between the cells I and $I+1$ are computed by using the MUSCL approach as [25]

$$U_{\mathrm{L}} = \bar{U}_I + \frac{1}{4}\left[\left(1+\hat{k}\right)\Phi^{-}_{I+\frac{1}{2}}\Delta_{I+\frac{1}{2}}\bar{U} + \left(1-\hat{k}\right)\Phi^{+}_{I-\frac{1}{2}}\Delta_{I-\frac{1}{2}}\bar{U}\right] \tag{1}$$

$$U_{\mathrm{R}} = \bar{U}_{I+1} - \frac{1}{4}\left[\left(1+\hat{k}\right)\Phi^{+}_{I+\frac{1}{2}}\Delta_{I+\frac{1}{2}}\bar{U} + \left(1-\hat{k}\right)\Phi^{-}_{I+\frac{3}{2}}\Delta_{I+\frac{3}{2}}\bar{U}\right] \tag{2}$$

where $\bar{U}$ is the cell-averaged value stored at a cell centre, $\Phi^{\pm}_{I\pm\frac{1}{2}}$ is a slope limiter, subscripts L and R represent the left and right states of the variable U across the cell-interface, and $\hat{k}$ is an integer that determines the stencil size. The expression $\Delta_{I+\frac{1}{2}}\bar{U}$ is evaluated as

$$\Delta_{I+\frac{1}{2}}\bar{U} = \bar{U}_{I+1} - \bar{U}_I \tag{3}$$

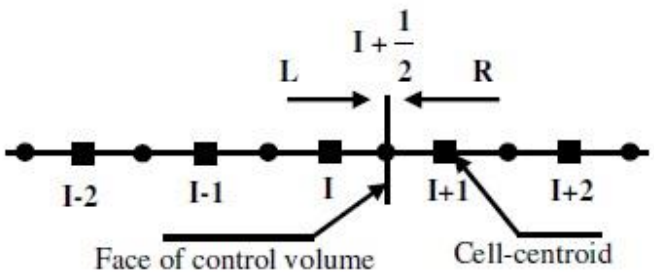

Figure 1. A cell-interface and its left and right states

In the case of van Albada limiter, $\hat{k}=0$ and the update equations for left and right states are given by [24]

$$U_{\mathrm{L}} = \bar{U}_I + \frac{1}{2}\delta_{\mathrm{L}} \tag{4}$$

$$U_{\mathrm{R}} = \bar{U}_{I+1} - \frac{1}{2}\delta_{\mathrm{R}} \tag{5}$$

where the function δ is typically the same for both the states given by

$$\delta = \frac{a\left(b^2+\varepsilon\right)+b\left(a^2+\varepsilon\right)}{a^2+b^2+\varepsilon} \tag{6}$$

so that

$$a_{\mathrm{R}} = \bar{U}_{I+2} - \bar{U}_{I+1},\ \mathrm{b}_{\mathrm{R}} = \bar{U}_{I+1} - \bar{U}_I \tag{7}$$

$$a_{\mathrm{L}} = \bar{U}_{I+1} - \bar{U}_{I},\ \mathrm{b}_{\mathrm{L}} = \bar{U}_{I} - \bar{U}_{I-1} \tag{8}$$

The additional parameter ε is required in order to prevent the activation of the limiter in smooth-flow regions owing to small-scale oscillations. It has to be set proportional to the local grid scale. Based on extensive numerical experiments the present work considers ε in terms of the cell volume V as

$$\varepsilon = 10 \times \left(V\right)^{1.25} \tag{9}$$

Inside the viscous-shear layers owing to the presence of physical diffusion the extrema in the flow field are attained smoothly. This offers an opportunity to switch off the slope limiter $\Phi^{\pm}_{I\pm\frac{1}{2}}$ inside the boundary layer, provided the presence of the boundary layer is sensed by a suitable sensor. If the slope limiter is switched off, the MUSCL reconstruction becomes

$$U_{\mathrm{L}} = \bar{U}_{I} + \frac{1}{4}\left[\left(1+\hat{k}\right)\Delta_{I+\frac{1}{2}}\bar{U} + \left(1-\hat{k}\right)\Delta_{I-\frac{1}{2}}\bar{U}\right] \tag{10}$$

$$U_{\mathrm{R}} = \bar{U}_{I+1} - \frac{1}{4}\left[\left(1+\hat{k}\right)\Delta_{I+\frac{1}{2}}\bar{U} + \left(1-\hat{k}\right)\Delta_{I+\frac{3}{2}}\bar{U}\right] \tag{11}$$

In order to regulate the slope limiter, a recently introduced boundary layer sensor is used in the present work. The boundary layer sensor r_{vg} is computed as the absolute ratio of velocity gradient across a cell-interface to the velocity gradient at the solid wall [18].

$$r_{\mathrm{vg}} = \left|\frac{\left(\partial U_{\mathrm{par}} / \partial\eta\right)_{\mathrm{interface}}}{\left(\partial U_{\mathrm{par}} / \partial\eta\right)_{\mathrm{wall}}}\right| \tag{12}$$

where U_{par} is the velocity component parallel to the wall and η is the direction normal to the wall. Literature suggests scaling down the numerical diffusion in the wall-normal direction only for viscous-flow computations [26]. Following the same principle, the present work also suggests to control the action of limiters in the higher-order-accurate computations of fluxes only across the cell-faces that are "aligned" with the flow. The algorithm for switching on and off the limiters for MUSCL reconstruction in the higher-order-accurate computations of fluxes is as follows:

(i) The parameter r_{vg} is used to track the location of the edge of the boundary layer. At the wall $r_{\mathrm{vg}}=1$. As one moves away from the wall towards the free stream, the value of the boundary-layer sensor decreases asymptotically till it attains a value zero far away from the wall. Thus, a critical height Y_{critical} is identified at the cell for which, $r_{\mathrm{vg}} \le 0.01$.

(ii) In the cells where $Y<Y_{\mathrm{critical}}$, the flow is considered to be inside the boundary layer, where physical viscosity plays a significant role. Therefore the limiter is switched off during the solution reconstructions within the boundary layer, and computations are carried out using Eq. (10) and Eq. (11).

(iii) For cells located at $Y \ge Y_{\mathrm{critical}}$ the solution reconstructions are done using Eq. (1) and Eq. (2). If the limiter used is van Albada, then these equations reduce to Eq. (4) and Eq. (5).

Numerical Simulation, Results and Discussion

In the present work, we choose to demonstrate the performance of higher-order-accurate AUSM scheme. The AUSM scheme is selected because of its high accuracy for viscous-flow computations. For illustration the solution reconstruction using the MUSCL approach with van Albada limiter is shown. However, our experience shows that the switching off other limiters inside the viscous-shear zones using the boundary-layer sensor also yield favourable results similar to that of the van Albada limiter. Two standard test cases are shown in the present paper, namely, viscous supersonic flow over an adiabatic flat plate at Mach 3 [18, 27, 28] and hypersonic flow over a ramped surface at Mach 6 [18, 28, 29]. The geometric and free-stream parameters for the two test cases are given in Table 1 and Table 2.

Table 1. The geometric and flow parameters for viscous supersonic flow over a flat plate

Parameter	Value
Length of the plate (L_c)	0.0000285 m
Free-stream pressure (p_∞)	101325 N/m^2
Free-stream temperature (T_∞)	288.15 K
Free-stream Mach number (M_∞)	3

Table 2. The geometric and flow parameters for hypersonic flow over a ramped surface

Parameter	Value
Length of the plate upto the compression corner (L_c)	0.05 m
Total length of the ramped surface	0.12 m
Ramp angle (θ)	15^0
Reynolds number per unit length $\mathrm{Re}_\infty \left(= \rho_\infty U_\infty / \mu_\infty\right)$	8X10^5 m^{-1}
Free-stream stagnation temperature	1747 K
Free-stream Mach number (M_∞)	6
Wall temperature (T_w)	298 K

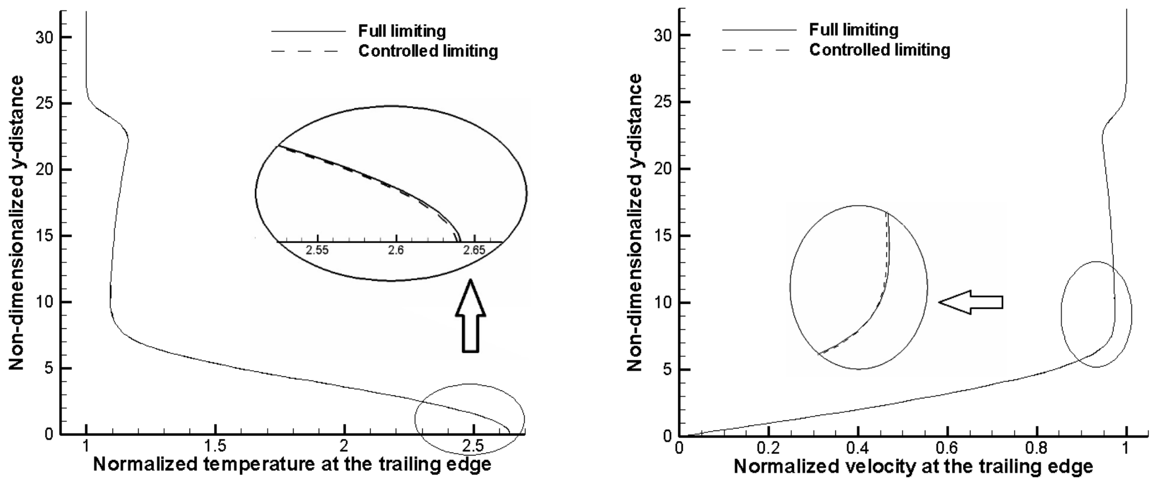

(a) (b)

Figure 2. Viscous supersonic flow over an adiabatic-flat plate: (a) temperature profile at the trailing edge (b) velocity profile at the trailing edge

The normalized-temperature (T/T_∞) profiles for viscous supersonic flow over a flat plate under the adiabatic condition are compared in Fig. 2(a). The *y*-distance is non-dimensionalized as suggested by Van Driest [30]. It can be seen that full limiting predicts a marginally higher adiabatic wall temperature compared with the controlled limiting. This is due to the fact that switching off the limiter inside the boundary layer during controlled limiting results in a lower level of numerical diffusion. The normalized-velocity profiles are shown in Fig. 2(b). As expected, the controlled limiting results in marginally less smearing of the hydrodynamic boundary layer, which is evident from the encircled and zoomed-in portions.

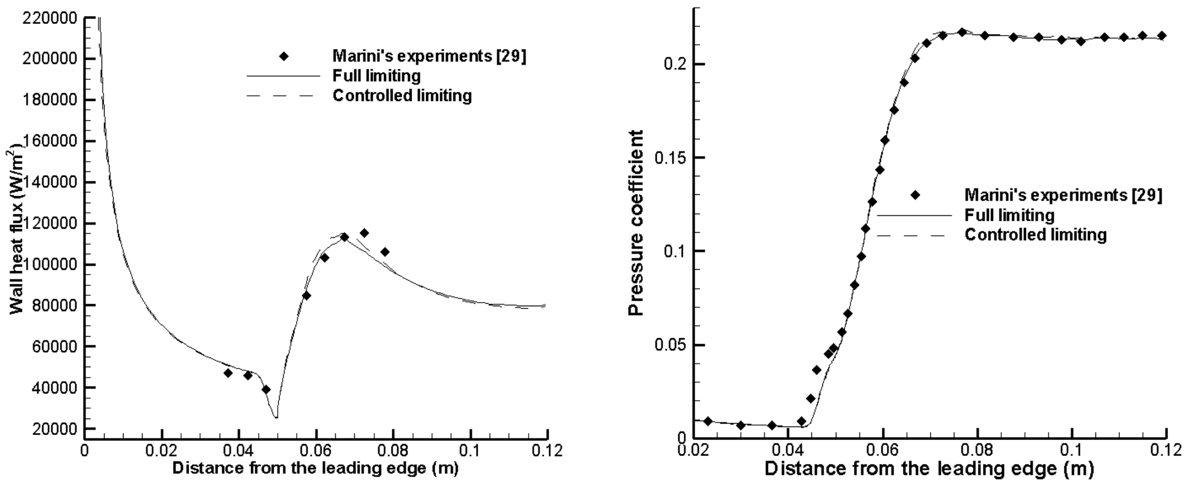

(a) (b)

Figure 3. Hypersonic flow over a ramped surface: (a) wall-heat flux along the surface (b) pressure coefficient along the surface

The variations of wall-heat flux from Marini's experimental results for hypersonic flow over a ramped surface are compared with the present computations in Fig. 3(a). With full limiting, the peak-heat flux in the post-reattachment zone is lower that the corresponding value with controlled limiting. In other words, the prediction of wall-heat flux with controlled limiting is in better agreement with the experimental results. The reason for this can be ascribed to the fact that full limiting induces more numerical diffusion compared with controlled limiting. Accordingly, both the computed hydrodynamic and thermal boundary layers are smeared more by the former case than the latter one. The increased smearing of the computed thermal boundary layer results in a lower temperature gradient at the wall, which leads to an under-estimation of the wall-heat flux. The variations of pressure coefficients with both full and controlled limiting are in close agreement with Marini's experiments, as can be seen in Fig. 3(b).

Conclusions

In the present work, a novel approach is proposed to control the diffusive action of limiters inside the boundary layers for computation of viscous compressible flows. The method proposes an algorithm to switch off the limiters inside the viscous shear layers and switch on the same in the inviscid zone using a recently introduced boundary-layer sensor. This is important since the viscous-flow computations demand the minimum possible level of numerical diffusion so as to avoid the smearing of hydrodynamic and thermal boundary layers. The superior performance of the approach is demonstrated by choosing the higher-order AUSM scheme with MUSCL reconstruction using van Albada limiter. Two standard test cases, namely, viscous supersonic flow over an adiabatic flat plate and hypersonic flow over a ramped surface are used to showcase the improved performance of the new approach. It is shown that controlling the diffusive effects of the limiters inside the boundary layers results in the decrease of smearing of boundary layers, thereby the improvement in accuracy of viscous-compressible-flow computations.

References

[1] van Leer B. (2006) Upwind and high-resolution methods for compressible flow: From donor cell to residual distribution schemes, *Communications in Computational Physics* , **1**, 192-206.

[2] Jaisankar S. and Raghurama Rao S.V. (2009) A Central Rankine-Hugoniot solver for hyperbolic conservation laws, *Journal of Computational Physics*, **228,** 770-798.

[3] Roe P.L. (1981) Approximate Riemann solvers, parameter vectors, and difference schemes, *Journal of Computational Physics*, **43** 357-372.

[4] van Leer B., Flux-vector splitting for the Euler equations, *Lecture Notes in Physics*, 1982, Springer-Verlag **170** 507-512.

[5] Liou M.S. and Steffen C.J. (1993) A new flux splitting scheme, *Journal of Computational Physics*, **107** 23-39.

[6] Nishikawa H. and Kitamura K. (2008) Very simple, carbuncle-free, boundary-layer-resolving, rotated-hybrid Riemann solvers, *Journal of Computational Physics*, **227** 2560-2581.

[7] Mesaros L.M., Multi-dimensional fluctuation splitting schemes for the Euler equations on unstructured grids, PhD Thesis, University of Michigan, 1995.

[8] Abgrall R. and Santis D.D. (2015) Linear and non-linear high order accurate residual distribution schemes for the discretization of the steady compressible Navier–Stokes equations, *Journal of Computational Physics*, **283** 329-359.

[9] Balsara D. S. (2010), Multidimensional HLLE Riemann solver: Application to Euler and magnetohydrodynamic flows, *Journal of Computational Physics*, **229** 1970-1993.

[10] Balsara D. S. (2012) A two-dimensional HLLC Riemann solver for conservation laws: Application to Euler and magnetohydrodynamic flows, *Journal of Computational Physics*, **231** 7476-7503.

[11] Balsara D. S. (2014) Multidimensional Riemann problem with self-similar internal structure. Part I–Application to hyperbolic conservation laws on structured meshes, *Journal of Computational Physics*, **277** 163-200.

[12] Dumbser M. and Balsara D. S. (2016) A new efficient formulation of the HLLEM Riemann solver for general conservative and non-conservative hyperbolic systems, *Journal of Computational Physics*, **304** 275-319.

[13] Lax P.D. (1954) Weak solutions of nonlinear hyperbolic equations and their numerical computation, *Communications on Pure and Applied Mathematics*, 7 159-193.

[14] Lax P.D. and Wendroff B. (1960) Systems of conservation laws, *Communications on Pure and Applied Mathematics*, **13** 217-237.

[15] LeVeque R.J. (2002) Finite Volume Methods for Hyperbolic Problems (Cambridge Texts in Applied Mathematics), Cambridge University Press.

[16] Jameson A., Schmidt W. and Turkel E., Numerical solutions of the Euler equations by finite volume methods using Runge-Kutta time stepping schemes, *AIAA paper*, 1981, paper 81-1259.

[17] van Leer B., Flux vector splitting for the 1990s, *Proceedings of Computational Fluid Dynamics Symposium on Aero-propulsion*, NASA, 1991, 203-214.

[18] Kalita P. and Dass A.K. (2016) A diffusion-regulated scheme for the compressible Navier-Stokes equations using a boundary layer sensor, Computers & Fluids **129** 91-100.

[19] Kalita P. and Dass A.K., Effect of numerical diffusion on the computation of hypersonic shock wave boundary layer interaction, *Proceedings of the International Symposium on Aspects of Mechanical Engineering & Technology for Industry*, North Eastern Regional Institute of Science and Technology India, 2014, 306-313.

[20] Godunov S.K. (1959) A difference scheme for numerical computation of discontinuous solutions of the equations of hydrodynamics, *Matematicheskii Sbornik* , **47** 271-306.

[21] van Leer B. (1979) Towards the ultimate conservative difference scheme V. A Second Order Sequel to Godunov Method, *Journal of Computational Physics*, **32** 101-136.

[22] Laney C.B. (1998) *Computational Gasdynamics*, Cambridge University Press.

[23] Jaisankar S. and Raghurama Rao S.V. (2007) Diffusion regulation for Euler solvers, *Journal of Computational Physics*, **221** 577-599.

[24] van Albada G.D., van Leer B. and Roberts W. W. (1982) A comparative study of computational methods in cosmic gas dynamics, *Astronomy and Astrophysics*, **108** 76-84.

[25] Blazek J. (2001) *Computational Fluid Dynamics; Principles and Applications*, 1st ed., Elsevier.

[26] Swanson R.C., Radespiel R. and Turkel E. (1998) On some numerical dissipation schemes, *Journal of Computational Physics*, **147** 518-544.

[27] Tu J., Yeoh G.H., and Liu C. (2007) *Computational Fluid Dynamics: A Practical Approach*, Butterworth-Heinemann.
[28] Kalita P. and Dass A. K. (2017) A novel hybrid approach with multidimensional-like effects for compressible flow computations, *Journal of Computational Physics*, **340** 55-68.
[29] Marini M., Effects of flow and geometry parameters on shock wave-boundary layer interaction in hypersonic flow, *AIAA paper*, 1998, paper 98-1570.
[30] Van Driest E.R. Investigation of laminar boundary layer in compressible fluids using the Crocco method, *NACA Technical Note*, 1952, paper 2597.